



LJMU Research Online

Aydin, E, Kloos, D-P, Gay, E, Jonker, W, Hu, L, Bullwinkel, J, Brown, JP, Manukyan, M, Giera, M, Singh, PB and Fundele, R

A hypomorphic Cbx3 allele causes prenatal growth restriction and perinatal energy homeostasis defects

<http://researchonline.ljmu.ac.uk/id/eprint/2555/>

Article

Citation (please note it is advisable to refer to the publisher's version if you intend to cite from this work)

Aydin, E, Kloos, D-P, Gay, E, Jonker, W, Hu, L, Bullwinkel, J, Brown, JP, Manukyan, M, Giera, M, Singh, PB and Fundele, R (2015) A hypomorphic Cbx3 allele causes prenatal growth restriction and perinatal energy homeostasis defects. JOURNAL OF BIOSCIENCES. 40 (2). pp. 325-338. ISSN

LJMU has developed [LJMU Research Online](http://researchonline.ljmu.ac.uk/) for users to access the research output of the University more effectively. Copyright © and Moral Rights for the papers on this site are retained by the individual authors and/or other copyright owners. Users may download and/or print one copy of any article(s) in LJMU Research Online to facilitate their private study or for non-commercial research. You may not engage in further distribution of the material or use it for any profit-making activities or any commercial gain.

The version presented here may differ from the published version or from the version of the record. Please see the repository URL above for details on accessing the published version and note that access may require a subscription.

For more information please contact researchonline@ljmu.ac.uk

<http://researchonline.ljmu.ac.uk/>

A hypomorphic *Cbx3* allele causes prenatal growth restriction and perinatal energy homeostasis defects

EBRU AYDIN¹, DICK-PAUL KLOOS², EMMANUEL GAY², WILLEM JONKER², LIJUAN HU¹,
JÖRN BULLWINKEL³, JEREMY P BROWN^{3,4}, MARIA MANUKYAN⁵, MARTIN GIERA², PRIM B SINGH^{3,4,6,*}
and REINALD FUNDELE^{1,*}

¹Sub-department of Evolution & Development, Center for Evolutionary Biology, Uppsala University,
Norbyvägen 18A, S-75236 Uppsala, Sweden

²Center for Proteomics and Metabolomics, Leiden University Medical Center (LUMC), Albinusdreef 2,
2300 RC Leiden, The Netherlands

³Division of Immunoepigenetics, Department of Immunology and Cell Biology, Research Center
Borstel, D-23845 Borstel, Germany

⁴Institute of Cell Biology and Neurobiology, Center for Anatomy, Charité-Universitätsmedizin Berlin,
Charitéplatz 1, D-10117 Berlin, Germany

⁵Albert-Ludwigs-Universität Freiburg, BIOSS Centre for Biological Signalling Studies,
Schänzlestrasse 18, 79104 Freiburg, Germany

⁶School of Natural Sciences and Psychology, Liverpool John Moores University, Byrom Street,
Liverpool L3 3AF, UK

*Corresponding author (PBS – Fax, +49-30-450-528902; Emails, prim.singh@charite.de and P.Singh@ljmu.ac.uk;
RF – Fax, +46-18-4716310, Email, rhf_devbiol@gmx.de)

Mammals have three HP1 protein isotypes HP1 β (CBX1), HP1 γ (CBX3) and HP1 α (CBX5) that are encoded by the corresponding genes *Cbx1*, *Cbx3* and *Cbx5*. Recent work has shown that reduction of CBX3 protein in homozygotes for a hypomorphic allele (*Cbx3*^{hypo}) causes a severe postnatal mortality with around 99% of the homozygotes dying before weaning. It is not known what the causes of the postnatal mortality are. Here we show that *Cbx3*^{hypo/hypo} conceptuses are significantly reduced in size and the placentas exhibit a haplo-insufficiency. Late gestation *Cbx3*^{hypo/hypo} placentas have reduced mRNA transcripts for genes involved in growth regulation, amino acid and glucose transport. Blood vessels within the *Cbx3*^{hypo/hypo} placental labyrinth are narrower than wild-type. Newborn *Cbx3*^{hypo/hypo} pups are hypoglycemic, the livers are depleted of glycogen reserves and there is almost complete loss of stored lipid in brown adipose tissue (BAT). There is a 10-fold reduction in expression of the BAT-specific *Ucp1* gene, whose product is responsible for non-shivering thermogenesis. We suggest that it is the small size of the *Cbx3*^{hypo/hypo} neonates, a likely consequence of placental growth and transport defects, combined with a possible inability to thermoregulate that causes the severe postnatal mortality.

[Aydin E, Kloos D-P, Gay E, Jonker W, Hu L, Bullwinkel J, Brown JP, Manukyan M, Giera M, Singh PB and Fundele R 2015 A hypomorphic *Cbx3* allele causes prenatal growth restriction and perinatal energy homeostasis defects. *J. Biosci.* **40** 325–338] DOI 10.1007/s12038-015-9520-x

1. Introduction

HP1 proteins are small adapter proteins that are constituents of larger complexes involved in a variety of nuclear

functions (Canzio *et al.* 2014). These include roles in heterochromatin formation, positive and negative transcriptional regulation, DNA repair, chromosome segregation and replication of heterochromatin (reviewed in Grewal and

Keywords. Brown adipose tissue; HP1; *Igf2P0*; placental development; *Ucp1*

Elgin 2007; Billur et al. 2010). In mammals, there are three HP1 isotypes, HP1 β (CBX1), HP1 γ (CBX3) and HP1 α (CBX5), that are encoded by distinct genes, chromobox homolog 1 (*Cbx1*), *Cbx3* and *Cbx5*, respectively (Jones et al. 2000). The three HP1 isotypes possess extensive sequence similarity, but this similarity belies their non-redundant functions. The suggestion that the mammalian HP1 isotypes are likely to possess non-redundant functions came first from immunolocalization studies using isotype-specific antibodies. CBX1 and CBX5 proteins were found to be concentrated at sites of constitutive heterochromatin (Saunders et al. 1993; Wreggett et al. 1994), while CBX3 was shown to have a more euchromatic distribution (Horsley et al. 1996). It was suggested that its euchromatic distribution reflected the acquisition of new functions by CBX3 and subsequently it was shown that CBX3 is associated with euchromatic genes and is involved in elongation and processing of their mRNA transcripts (Vakoc et al. 2005; Hediger and Gasser 2006; Smallwood et al. 2012).

Proof that HP1 isotypes were non-redundant came from mutational analyses. It was demonstrated that loss of CBX1 protein cannot be compensated by CBX3 and CBX5 proteins (Aucott et al. 2008) because the murine *Cbx1*^{-/-} mutation is perinatal lethal. Mortality is caused by respiratory failure due to defective post-synaptic differentiation in the diaphragm (Aucott et al. 2008). In addition, while other organ systems seemed intact, *Cbx1*^{-/-} mutants exhibited defective development of the central nervous system that was associated with a profound genomic instability (Aucott et al. 2008). Deletion of the CBX5 protein had no obvious effect. *Cbx5*^{-/-} mice are fully viable and fertile (cited in Aucott et al. 2008), indicating a redundancy, most likely with CBX1. However, a recent study has shown that *Cbx5*^{-/-} mice exhibit a specific defect in the silencing of T_H1 expression in T_H2 cells (Allan et al. 2012). These data show that CBX protein function(s) are likely to be overlapping, but there are non-redundant functions peculiar to each isotype that cannot be compensated and some of these functions may be quite specific in character.

Ablation of *Cbx3* expression causes infertility in both sexes and a severe neonatal mortality (Brown et al. 2010; Abe et al. 2011; Takada et al. 2011). In one study, which used a hypomorphic *Cbx3* allele (*Cbx3*^{hypo}), roughly 99% of the homozygous mutants died before weaning, whereas on day 19 of fetal development (E19) normal Mendelian ratios of wild-type to targeted alleles were observed (Brown et al. 2010). In all *Cbx3*^{hypo/hypo} tissues examined the levels of CBX3 protein were barely detectable (Brown et al. 2010). The causes for the neonatal demise of *Cbx3*^{hypo/hypo} homozygotes are not known. Here we describe the cellular and molecular changes that take place in *Cbx3*^{hypo/hypo} conceptuses and newborns. Our findings indicate that the *Cbx3*^{hypo/hypo} mutation is pleiotropic and causes generalized defects in

placental development and energy homeostasis that are together responsible for the postnatal mortality of *Cbx3*^{hypo/hypo} homozygotes.

2. Materials and methods

2.1 Mice and mouse tissues

All experiments with mice were conducted according to the guidelines issued by Uppsala University. The *Cbx3*^{hypo} allele, which has been described in detail in Brown et al. (2010), was propagated as heterozygote in a mixed C57BL6/129 genetic background at the Borstel Research Center and subsequently at the animal facilities at the Biomedical Center, Uppsala, where the allele was crossed into a BALB/c background to backcross 3. No obvious differences could be observed between fetuses from matings with different strain combinations and consequently results are pooled. Pregnant females were killed by cervical dislocation, with the day of vaginal plug being counted as day 1. Fetuses and placentas were weighed. Placentas were halved, one half was frozen on dry ice for nucleic acid or protein extraction, while the other half was either fixed in Carnoy's fixative and later processed for paraffin histology, or embedded directly in Tissue-Tek O.C.T. Compound (Sakura) and used for cryo-sectioning. For determination of blood glucose levels, newborn mice were decapitated and blood glucose determined with a OneTouch UltraEasy glucose meter.

2.2 BrdU cell proliferation assay

Cellular proliferation in placental and fetal tissues was determined using the BrdU assay according to Jägerbauer et al. (1992).

2.3 Staining of sections

Antibodies used were against smooth muscle actin (DAKO M0851) and BrdU (DAKO M0744), isolectin B4 was obtained from Vector laboratories (B-1205). Horseradish peroxidase-labelled secondary antibodies were obtained from DAKO and Vector laboratories. IHC was carried out according to standard procedures. Antigen retrieval was performed in a microwave at 480 W for 10 min in 10 mM citrate, 0.05% Tween20, pH 6.0. Frozen, 10% PFA post-fixed sections were stained with Oil red O. Carnoy's fixed paraffin sections were stained with PAS. For counting of nuclei, pictures were taken at 40 \times magnification and quantified on a screen. Three randomly selected areas from at least 3 different fetuses were analysed.

2.4 DNA extraction and genotyping PCR

Genomic DNA was extracted from tissues using the Promega Wizard genomic DNA extraction kit. The following primers were used to genotype *Cbx3* mutant mice: forward: 5'-AGTCCCAGTACTGAGAGTTC-3' and reverse: 5'-CTCTACCTCCTGAGTACTAG-3'. Reaction conditions have been described previously (Brown *et al.* 2010).

2.5 Lipid extraction and analysis

For placental transport analysis (Wu *et al.* 2003; Yu *et al.* 2008), total lipid was extracted and purified from *Cbx3*^{hy^{po}/hy^{po}} and *Cbx3*^{+/+} E13 and E18 fetuses and their placentas and the ratios of EFAs (20:4; 18:2; 22:6) to NEFAs (16:0; 18:0) were determined. BSTFA containing 1% TMCS was from Thermo (Runcorn, UK). All other chemicals were from Sigma Aldrich (Schnellendorf, Germany). A Scion TQ GC-MS system from Bruker (Bremen, Germany) equipped with a Bruker BR5-MS 15 m × 0.25 mm × 0.25 μm column was used. The injector was operated in splitless mode, held at 280°C. The injection volume was 1 μL and the oven program started and kept for 0.5 min at 90°C, ramped to 180 with 30°C/min, then to 250°C with 10°C/min, then to 266°C with 2°C/min, and finally to 300°C with 120°C/min. Helium (99.9990%) was used as carrier gas at a flow rate of 1.2 mL/min. The retention times of all analytes were determined, so the selected ion monitoring (SIM) method could be programmed with a 0.30 min window for each compound.

For the analysis of the total lipid content, to ~1 mL sample, 3 mL of methanol and 1 mL of 10 M NaOH were pipetted into a pre-cleaned glass 10 mL test-tube. Before closing the tube, the atmosphere in the vial was flushed with argon. The tube was placed in an oven for 1 h at 90°C. After cooling, 2 mL of 6 N of HCl were added, subsequently 10 μL internal standard (C16:0 d31) was added. Extraction was carried out by adding 3 mL of *n*-hexane. After shaking, the *n*-hexane layer was transferred to another tube. This was done three times, to ensure an optimal extraction. *n*-Hexane was added to the extract to 10 mL. 50 μL were taken from the extract and dried in an autosampler vial.

Dried samples were derivatized by 25 μL of MtBSTFA for 10 min at room temperature and subsequently 25 μL of BSTFA and 2.5 μL of pyridine were added before putting the sample in an oven for 15 min at 50°C. 947.5 μL of *n*-hexane, containing 10 μg/mL octadecane (C18) internal standard, was used to dilute the sample, prior to injection.

2.6 Quantitative real-time RT-PCR (qRT-PCR)

Gene expression levels were analysed by quantitative real time PCR (Corbett Research RG-3000 thermo-cycler) for the growth regulatory genes (*Grb10*, *Igf2*, *H19*), the placenta-specific transcript of *Igf2* (*Igf2P0*), the placental transporter genes of the system A family of amino acid transporters (*Slc38a1*, *Slc38a2*, *Slc38a4*), the predominant placental glucose transporters (*Slc2a1*, *Slc2a3*), the prolactin family genes (*Prl*, *Prlr*, *Prl7b1*, *Prl3c1*, *Prl4a1*, *Prl8a9*, *Prl7c1*), the key enzymes in glucose homeostasis (*G6pc*, *Pck1*, *Gys2*), and the genes related to lipid and mitochondrial metabolism (*Pparg2*, *Srebp1*, *Pgc1a*, *Ucp1*, *Cs*, *Hmgcs1*). Total RNA was extracted from snap-frozen tissues with TRIzol reagent (Ambion Life Technologies) according to manufacturer's guide. DNase treatment was performed prior to cDNA synthesis with Promega's RQ1 RNase-Free Dnase Kit. cDNA was synthesized using high-capacity cDNA Reverse Transcription Kit of Applied Biosystems. PowerSYBR® Green PCR Master Mix (Life Technologies) was used for real time PCR quantification of transcripts. All samples were analysed in triplicates and data were normalized using Delta Delta CT method (Livak and Schmittgen, 2001). Accordingly, the amplification efficiency of the constitutively expressed reference genes, *Tubb*, *Actb* and 28s rRNA, were compared of the amplification of the target genes of interest (given above) in order to find the optimal combination of reference gene and target gene for calculation of normalized expression as described by Livak and Schmittgen (2001).

Conditions and primer sequences used in qRT-PCR are shown in the table below.

Gene	Forward Primer (5' → 3')	Reverse Primer (5' → 3')	Annealing Temp	Product Size(bp)
<i>Pparg2</i>	GCATCAGGCTTCCACTATGGA	AAGGCACTTCTGAAACCGACA	60	161
<i>Prlr</i>	TGGTGAATCCTGGGTCAGA	CTTCCATTTCGTTCGTGGC	58	194
<i>Srebp1</i>	CGGCTGTTGTCTACCATAAGCTG	CATAGATCTCTGCCAGTGTTGCC	58	152
<i>Pgc1a</i>	CCCAGGCAGTAGATCCTCTTCAA	CCTTTCGTGCTCATAGGCTTCATA	58	162
<i>Ucp1</i>	TCTGCATGGGATCAAACCCC	ACAGTAAATGGCAGGGGACG	58	215
<i>Igf2</i>	CGCTTCAGTTTGTCTGTTCG	GCAGCACTCTTCCACGATG	58	95
<i>Cs</i>	TGTTTCAGGGCCTTTAAGACT	CATGCTTCAGTCCC GGTCAT	63	181
<i>Hmgcs1</i>	CCTGGCACAGTACTCACCTC	AGCCAAGCCAGAACCGTAAG	59	73

<i>G6pc</i>	CTGCTGTGTCTGGTAGGCAA	CCTGGGTCTCCTTGCCATTT	59	91
<i>Pck1</i>	TTGAACTGACAGACTCGCCC	GGCACTTGATGAACTCCCCA	63	105
<i>Gpd1</i>	CAGGTCCCTCTCTGCTCCTA	CCAGTCGGGATCGATGACAG	62	102
<i>Atg5</i>	AGTGGAGGCAACAGAAACCC	TCCTGTGTGTCTCAGCGAAG	58	115
<i>Atg7</i>	TGCCTATGATGATCTGTGTC	CACCAACTGTTATCTTTGTCC	54	146
<i>Gys2</i>	CTCTCCTGAAAGGCAGCAAGG	ACAGGGTGAGCCAGCAATC	60	85
<i>Cbx3</i>	TGAAGTGGAAGGACTCGGAC	GTAATTCAAAAACCCAAGATCCAGA	58	200
<i>Prlpn</i>	GGACACCAGTTTAGCAGCCT	GTCTTCGGTGAGCATTTCGC	59	197
<i>Prl3c1</i>	AAAGTCGTTCTGGAGGGAGC	TTTTGCCATGCTTCAGAGCC	62	211
<i>Prl4a1</i>	GACCACCAGATGCCACACTT	TGGATCCCAGCCTTTCACAC	62	164
<i>Prl8a9</i>	CAGCTGGAACCTTCGTACA	ATCTGCATGCTCAGTTCCCC	62	188
<i>Prl7c1</i>	GCTGCCACACATTTCCCTC	GTTTAGGGTCTCGATGGCGT	56	200
<i>Igf2p0</i>	CTTCAGGAACTACGAAGCGACT	GTCGTCGTAGTCGTTCTCCTCT	58	101
<i>Slc2a1</i>	AGCATCTTCGAGAAGGCAGG	ACAACAAACAGCGACACCAC	58	98
<i>Slc38a4</i>	AGGGCTGTGAGGTCAAATGG	AAATTGGCTGTTTCATGGCGTC	58	142
<i>Slc38a1</i>	CTTGCTACACGAGTGGGTT	TGTCGAGTCTGCTCCACAC	58	108
<i>Slc38a2</i>	CATCCGCTGTTCTTCCCAT	CCGATTCCACGTGTCGGTAA	58	154
<i>Grb10</i>	GGACAAAGTGGGGCAGTCAA	GGCTTCCACGGACGAGTTA	58	140
<i>Slc2a3</i>	GAACACTTGCTGCCGAGAAC	AGATGGGGTACCTTCGTTG	58	100

3. Results

3.1 Effect of the *Cbx3*^{hypo} allele on placental and fetal growth

Placental and fetal weights were determined between E12 and E19 (figure 1). At E12 *Cbx3*^{hypo/hypo} homozygous placentas exhibited a tendency for reduced weight, compared to both *Cbx3*^{hypo/+} and *Cbx3*^{+/+} placentas (figure 1c). From day 13 onwards weight differences between *Cbx3*^{hypo/hypo} and *Cbx3*^{+/+} placentas were statistically highly significant ($P < 0.001$; figure 1c), with the mean relative weight of the *Cbx3*^{hypo/hypo} placentas reaching a minimum at E14 and E16, with 62.1% and 62.0% of wild-type weights respectively. There was some catch-up on E18 and E19 where mean relative weights of *Cbx3*^{hypo/hypo} placentas reached 70.4% and 74.8% of wild-type placentas respectively. Notably, *Cbx3*^{hypo/+} placenta weights were consistently intermediate between *Cbx3*^{hypo/hypo} and *Cbx3*^{+/+} (figure 1c), indicating that the *Cbx3*^{hypo} allele is haplo-insufficient with regard to placental weight. Specifically, the weight differences between *Cbx3*^{hypo/hypo} and *Cbx3*^{hypo/+} placentas were significant at all stages except E12 ($P < 0.05$ for E13, $P < 0.001$ for all other stages); between *Cbx3*^{hypo/+} and wild-type placentas, weight differences were significant on E13 ($P < 0.005$), E18 ($P < 0.01$), and E19 ($P < 0.01$). With regard to fetal weights, the weights of *Cbx3*^{hypo/hypo} fetuses were significantly reduced compared with both *Cbx3*^{hypo/+} and *Cbx3*^{+/+} fetuses from day 16 onwards (figure 1d).

These data indicate that the reduced placental weights we observed from day 13 (figure 1c) could cause or contribute

to the fetal growth restriction that follows. *Cbx3*^{hypo/hypo} fetuses showed no catch-up growth during late gestation unlike *Cbx3*^{hypo/hypo} placentas. Neither was there any significant weight difference between *Cbx3*^{hypo/+} and *Cbx3*^{+/+} fetuses at any stage (figure 1d), showing that the *Cbx3* haplo-insufficiency was only in the placenta.

3.2 Effect of the *Cbx3*^{hypo} allele on proliferation in placental and fetal tissues

It is known that differential cell proliferation is sufficient to explain growth phenotypes (Zechner et al. 2002). To determine if reduced fetal and placental weights were caused by decreased cell proliferation, we performed anti-BrdU immunohistochemistry (IHC) and calculated the percentage of BrdU-positive nuclei.

With regard to fetuses there was clear evidence for decreased proliferation in *Cbx3*^{hypo/hypo} vs. *Cbx3*^{+/+} tissues at E13, with 18.5±3.0% vs. 32.9±4.1% BrdU-positive nuclei in heart (figure 2a and b; $P = 0.001$), 38.9±3.7% vs. 47.2±4.9% BrdU-positive nuclei in lung ($P = 0.001$), and 27.7±2.9% vs. 31.2±1.6% in tongue ($P < 0.002$). On E18 no significant difference could be observed between hearts of *Cbx3*^{hypo/hypo} and wild-type fetuses (22.5±0.76 vs. 23.0±0.99; $P = 0.57$). Notably, at E18 the brown adipose tissue (BAT) of *Cbx3*^{hypo/hypo} fetuses exhibited significantly increased BrdU-incorporation compared to wild-type BAT (figure 2c and d; 16.7±5.3% vs. 6.8±4.7%; $P < 0.001$).

With regard to the placenta, decreased proliferation was observed in the E13 *Cbx3*^{hypo/hypo} labyrinth, which

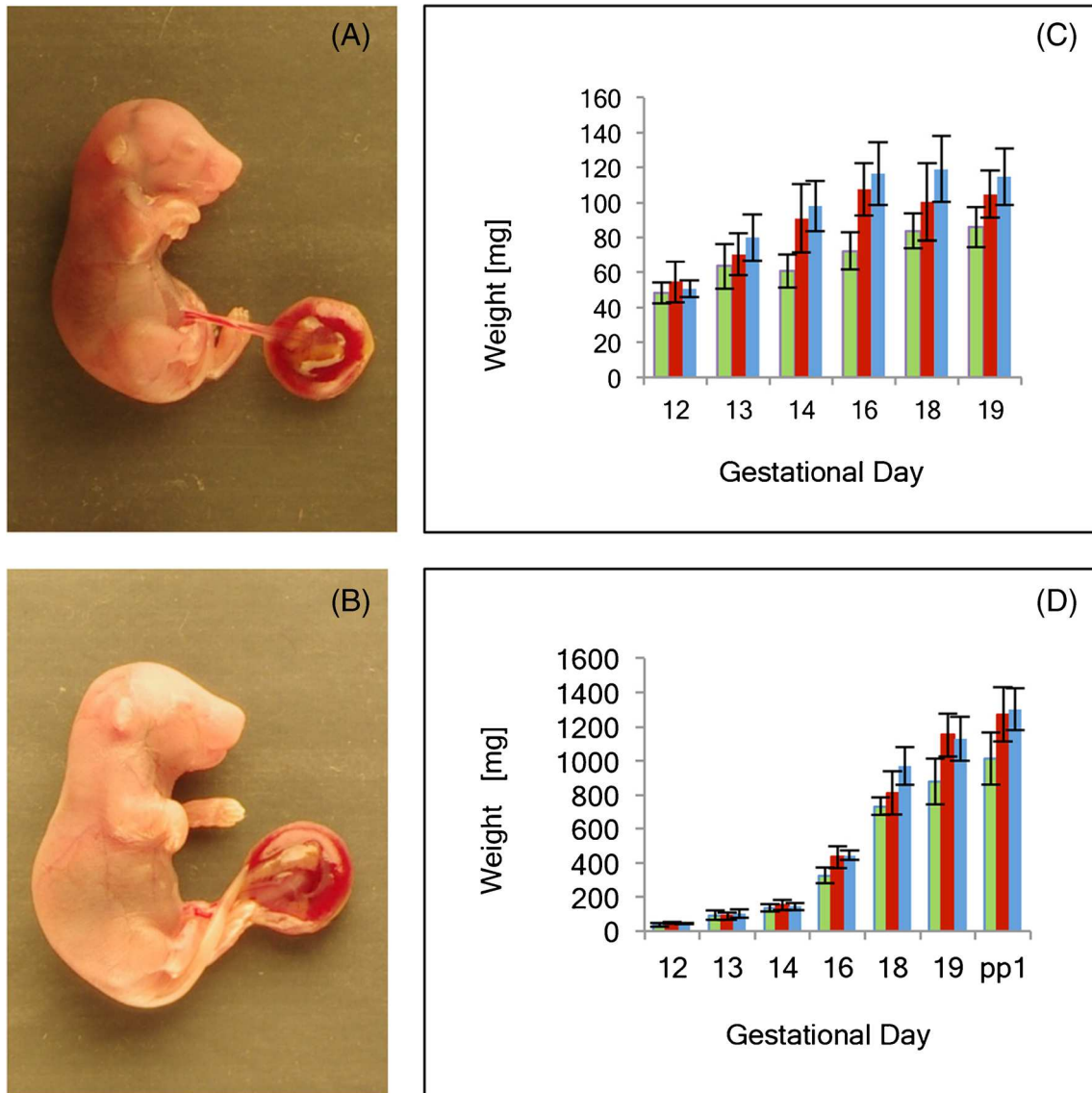


Figure 1. Homozygosity for *Cbx3*^{hypo/hypo} causes placental and fetal growth restriction. (a) An E19 *Cbx3*^{hypo/hypo} conceptus whose placental and fetal weights were 84.1 and 752 mg respectively. (b) An E19 *Cbx3*^{hypo/+} conceptus whose placental and fetal weights were 107 and 1095 mg respectively. We have shown the comparison of the *Cbx3*^{hypo/hypo} conceptus in (a) with the E19 *Cbx3*^{hypo/+} conceptus in (b) so that the similarity in size of the placentas can be seen, which is where the haplo-insufficiency for *Cbx3*^{hypo} is observed. By contrast there is an obvious difference in size of the fetuses. (c) Diagram of the weight increase of *Cbx3*^{hypo/hypo}, *Cbx3*^{+/+} and *Cbx3*^{+/+} placentas between E12 and E19 of gestation; values are shown as $\bar{x} \pm S.D.$ (d) Diagram of the weight increase of *Cbx3*^{hypo/hypo}, *Cbx3*^{+/+} and *Cbx3*^{+/+} fetuses between E12 and E19 of gestation and for *post partum* day 1 (PP1) newborn mice; values are shown as $\bar{x} \pm S.D.$ Statistical significance was assessed by unpaired *t*-test. Number of conceptuses: E12 - hypo/hypo=4; hypo/+ =7; +/+ =5; E13 - hypo/hypo=16; hypo/+ =53; +/+ =25; E14 - hypo/hypo= 9; hypo/+ =18; +/+ =8; E16 - hypo/hypo=8; hypo/+ =18; +/+ =9; E18 - hypo/hypo= 10; hypo/+ =23; +/+ =12; E19 - hypo/hypo=25; hypo/+ =61; +/+ =22; PP1 - hypo/hypo= 13; hypo/+ =24; +/+ =15; hypo/hypo=*Cbx3*^{hypo/hypo}; hypo/+ =*Cbx3*^{hypo/+}; +/+ =*Cbx3*^{+/+}; green bars=*Cbx3*^{hypo/hypo}; red bars=*Cbx3*^{hypo/+}; blue bars=*Cbx3*^{+/+}.

had $38.7 \pm 5.1\%$ BrdU-positive nuclei as compared to $51.5 \pm 10.8\%$ in wild-type labyrinth ($P < 0.001$). The E13 spongiotrophoblast, the supporting structure of the developing labyrinthine layer, showed no significant differences in cell proliferation (8.7 ± 4.3 wt vs. 11.5 ± 3.3 *Cbx3*^{hypo/hypo}; $P = 0.09$).

3.3 Placental morphology and function

Prompted by the observation that placental growth restriction presaged the onset of fetal growth restriction (figure 1) and may thus cause the fetal growth restriction, we decided to

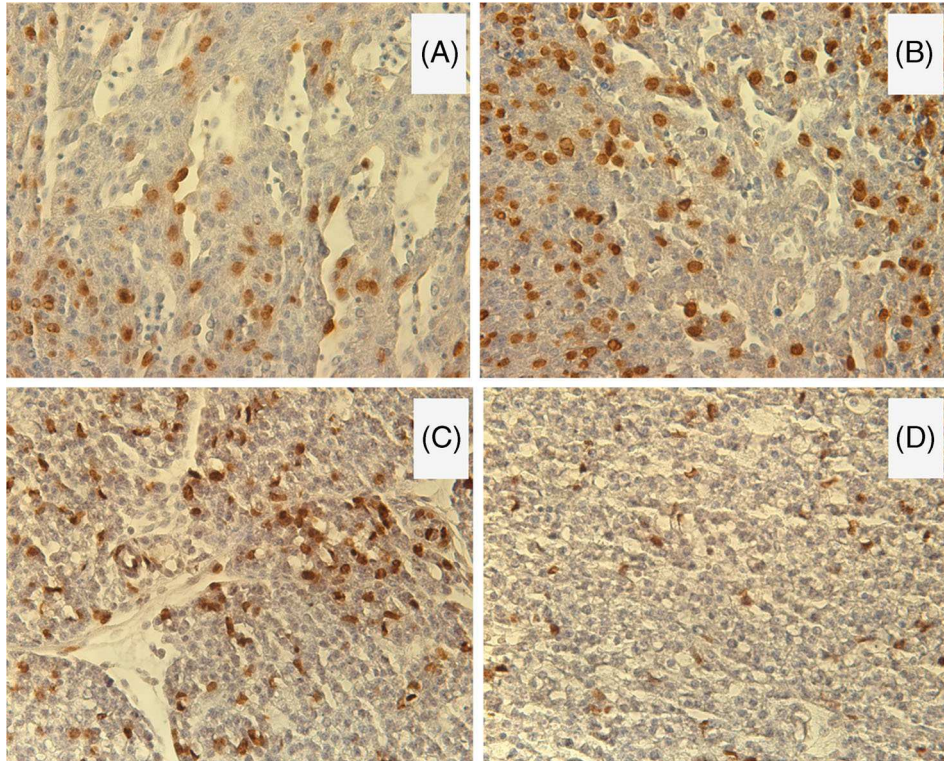


Figure 2. Cellular proliferation in $Cbx3^{\text{hypo/hypo}}$ and $Cbx3^{+/+}$ fetal tissues. Cellular proliferation was determined by BrdU-IHC. (a) BrdU-IHC on a section of E13 $Cbx3^{\text{hypo/hypo}}$ heart. (b) BrdU-IHC on a section of E13 $Cbx3^{+/+}$ heart that is a littermate of the fetus in (a). Comparison of (a) with (b) shows that there is reduced BrdU incorporation in the $Cbx3^{\text{hypo/hypo}}$ heart. (c) BrdU-IHC on a section of E18 $Cbx3^{\text{hypo/hypo}}$ BAT. (d) BrdU-IHC on a section of E18 $Cbx3^{+/+}$ BAT that is a littermate of the fetus in (c). Comparison of (c) with (d) shows that there is increased BrdU incorporation in the $Cbx3^{\text{hypo/hypo}}$ BAT. Number of tissues counted: hypo/hypo=4; +/+ =4; three areas were analysed from each tissue. Magnifications are $\times 40$ of the original.

investigate placental morphology and function in more detail. We compared the placental morphology of $Cbx3^{\text{hypo/hypo}}$ and wild-type placentas between E12 and E19 of gestation using hematoxylin and eosin (HE), an anti-smooth muscle actin (SMA) antibody and isolectin-B4 (BSB4) that marks the matrix surrounding fetal blood vessels (Wood *et al.* 1979; Kurz *et al.* 1999).

We did not observe any consistent alterations of placental morphology in early post-mid gestation $Cbx3^{\text{hypo/hypo}}$ placentas, but we did observe some changes in late gestation $Cbx3^{\text{hypo/hypo}}$ placentas. First, as shown in figure 3a to d, we observed increased staining, both in terms of the numbers of cells and staining intensity, of the SMA-positive pericytes. Apart from this enhanced staining of pericytes smooth muscle differentiation looked normal in late gestation $Cbx3^{\text{hypo/hypo}}$ placentas. Second, there was decreased BSB4-staining (*C.f.* figure 3e with 3f) that was associated with decreased width of blood vessels. Third, we observed increased numbers of nuclei per given area in sections of late gestation $Cbx3^{\text{hypo/hypo}}$ placentas compared to wild-type placentas. E18 and E19 $Cbx3^{\text{hypo/hypo}}$ placental sections showed significantly

higher nuclear density in the labyrinth compared to wild-type placentas (E18: 291 ± 35.3 vs. 257 ± 35.6 ; E19: 315 ± 51 vs. 206 ± 42 ; $P < 0.001$; *C.f.* figure 3i with 3j). This contrasted to the situation found at E12 where nuclear density in the labyrinth was reduced in $Cbx3^{\text{hypo/hypo}}$ compared to wild-type placentas (231 ± 16 vs. 273 ± 17 ; $P = 0.02$; *C.f.* figure 3g with 3h); analysis of intervening stages showed that the tendency for reduced nuclear density in $Cbx3^{\text{hypo/hypo}}$ labyrinth persisted until E14. These findings indicate that after E14 the $Cbx3^{\text{hypo/hypo}}$ placentas compensate by increasing cell number and thus the surface area for exchange of nutrient, gas and waste exchange between the fetal and maternal blood supplies.

We next measured changes in mRNA transcripts of genes whose expression is known to change during the placental growth restriction that results from undernourishment of dams (Coan *et al.* 2010). They included placental growth regulators, amino acid and glucose transporters (figure 3k). In E19 $Cbx3^{\text{hypo/hypo}}$ placentas expression of the placenta-specific transcript of *Igf2*, *Igf2P0*, and of *Grb10* are reduced

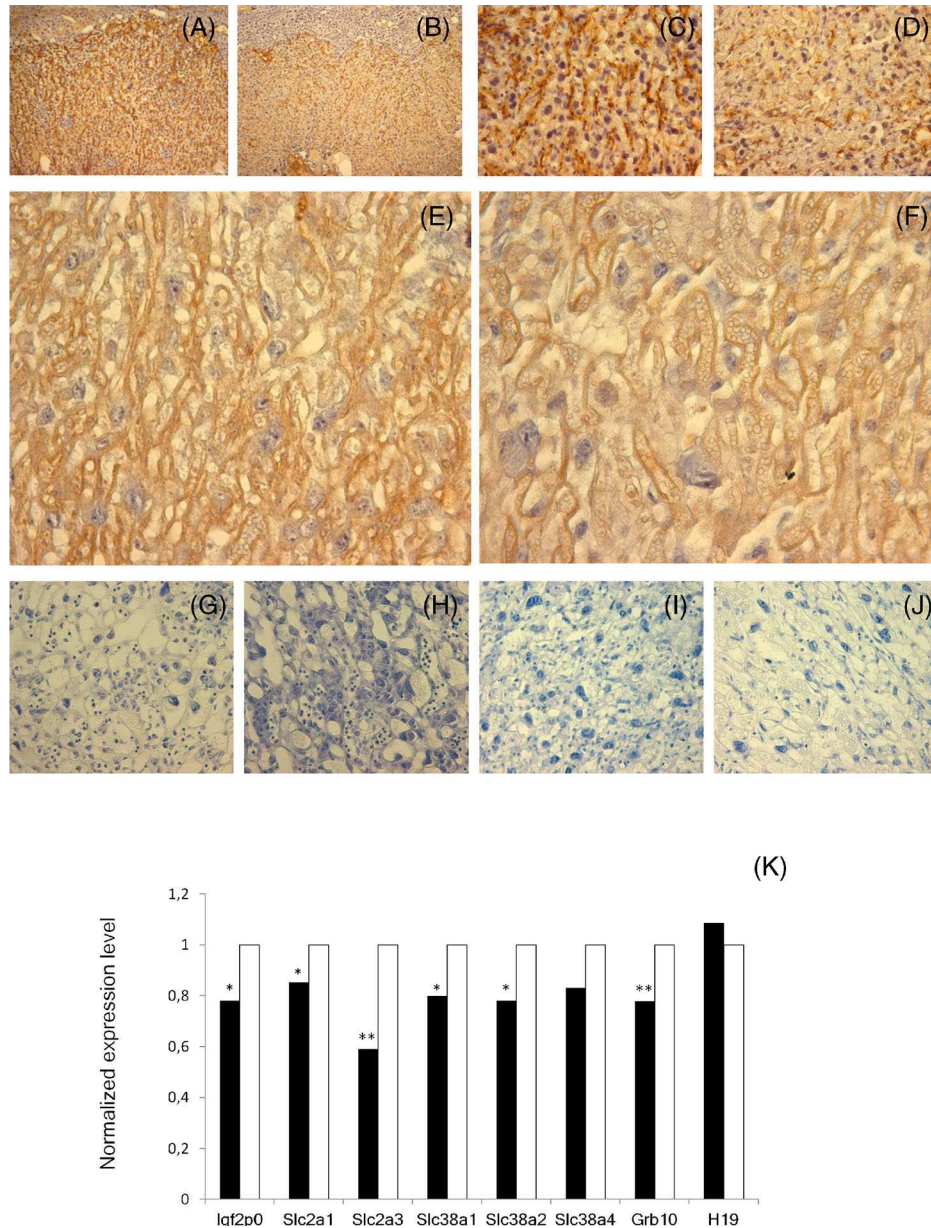


Figure 3. Altered placental morphology of *Cbx3*^{hypohypoplasia} placentas. Morphology of placentas was investigated using anti-smooth muscle actin (SMA) and Isolectin BSB4 IHC. (a, c) Anti-SMA IHC on placental sections of E19 *Cbx3*^{hypohypoplasia}. (b, d) Anti-SMA IHC on placental sections of E19 *Cbx3*^{+/+} that is a littermate of the animal in (a, c). Comparison of (a, c) with (b, d) shows that there both an increase in the number and in the intensity of staining of the SMA-positive pericytes in *Cbx3*^{hypohypoplasia} placentas. (e) Isolectin BSB4-staining of E19 *Cbx3*^{hypohypoplasia} placenta. (f) Isolectin BSB4-staining of E19 *Cbx3*^{+/+} placenta. Comparison of (e) and (f) shows decreased width of blood vessels in *Cbx3*^{hypohypoplasia} placentas. Number of placentas analysed: hypo/hypo=6; +/+ =6. (g to j) The nuclei of E12 to E19 placental sections from *Cbx3*^{hypohypoplasia} and *Cbx3*^{+/+} littermates were stained and counted. Comparing the number of nuclei in E12 *Cbx3*^{hypohypoplasia} (g) placentas to that of *Cbx3*^{+/+} (h) littermates showed that the nuclear density was reduced in E12 *Cbx3*^{hypohypoplasia} placentas (number of placentas counted: hypo/hypo=2; +/+ =2; 3 areas were analysed from each placenta). By contrast, E19 *Cbx3*^{hypohypoplasia} placentas shown in (i) exhibited higher nuclear density in the labyrinth than *Cbx3*^{+/+} littermates shown in (j) (number of placentas analysed: hypo/hypo=4; +/+ =2; 3 areas were analysed from each placenta). (k) Normalized real time PCR transcripts of genes relevant to placental growth and transport function. mRNA transcripts in *Cbx3*^{hypohypoplasia} placentas were measured on E19 (black, filled bars) and compared to *Cbx3*^{+/+} transcript levels that were normalized to 1.0 (empty bars). Significant expression changes are indicated by asterisks (**p*< 0.05; ***p*<0.01). Statistical significance was assessed by unpaired *t*-test. *Cbx3*^{hypohypoplasia} gene expression levels are indicated by filled bars, *Cbx3*^{+/+} levels, normalized to 1.0, by empty bars (number of placentas analysed: hypo/hypo=3; +/+ =3). Magnification in (a, b) is ×10 and (c to j) is ×40 of the original.

to 78% and 70% of wild-type respectively. There was no significant change in expression of the growth regulator H19. E19 $Cbx3^{hypo/hypo}$ placentas showed significantly reduced expression of mRNA transcripts in two of the three members of the system A amino acid transporter family, $Slc38a1$ (down to 80% of wt) and $Slc38a2$ (down to 78% of wt). There was no significant change in the expression of the $Slc38a4$ gene. There was a dramatic reduction in the mRNA transcript of placental glucose transporter gene, $Slc2a3$, to 58% of wild-type levels. The $Slc2a1$ mRNA transcript was also reduced to 83% of wild-type levels.

To directly test placental transport function we determined essential fatty acid (EFA) transport across the placenta. We used the method detailed in Wu *et al.* (2003) and Yu *et al.* (2008) and measured fetal and placental ratios of EFAs: non-essential FAs (NEFAs) in $Cbx3^{hypo/hypo}$ and wild-type littermates at E13 and E18. At E13 there was no significant difference in placental EFA:NEFA ratios in two litters that were investigated. In one of the E13 litters there was a significantly reduced EFA:NEFA ratio in the fetuses, with values of 1.67 ± 0.21 in $Cbx3^{hypo/hypo}$ (N=2) vs. 2.44 ± 0.21 in wild-type and heterozygous (N=3; $P < 0.05$). However, fetuses of the second E13 litter showed no significant differences, with EFA:NEFA ratios of 3.23 ± 0.04 in $Cbx3^{hypo/hypo}$ (N=2) vs. 2.98 ± 0.21 in control littermates (N=2). Examination of an E18 litter, which comprised two $Cbx3^{hypo/hypo}$ fetuses and four wild-type and heterozygous controls, showed that the EFA:NEFA ratios were significantly reduced in the heads of the $Cbx3^{hypo/hypo}$ fetuses (1.83 ± 0.12 vs. 2.51 ± 0.14 ; $P = 0.02$), but not in the rest of the bodies (2.15 ± 0.21 vs. 2.65 ± 0.69 ; $P = 0.16$) or in the placentas.

3.4 Newborn $Cbx3^{hypo/hypo}$ mutants do not exhibit major morphological abnormalities

We have previously shown that roughly 99% of $Cbx3^{hypo/hypo}$ homozygotes on a mixed 129/Sv-C57BL/6 genetic background die before weaning, whereas during prenatal development normal Mendelian ratios of $Cbx3^{hypo}$ to wild-type alleles were observed (Brown *et al.* 2010). The nature and the timing of the postnatal attrition of $Cbx3^{hypo/hypo}$ homozygotes was not determined (Brown *et al.* 2010). A number (N=10) of post-partum (PP1) day 1 litters from $Cbx3^{hypo/+} \times Cbx3^{hypo/+}$ matings were analysed. The prenatal fetal weight restriction (figure 1) persisted in postnatal $Cbx3^{hypo/hypo}$ pups. At PP1 $Cbx3^{hypo/hypo}$ body weights were 79% of $Cbx3^{hypo/+}$ and $Cbx3^{+/+}$ combined ($P < 0.001$; figure 1d). When a PP8 litter consisting of four pups was analysed, body weights were 3,805 and 3,288 mg for $Cbx3^{hypo/hypo}$ and 5,657 mg and 5,756 mg in a $Cbx3^{+/+}$ and a $Cbx3^{hypo/+}$, respectively; $Cbx3^{hypo/hypo}$ weights were 62% of wild-type. Reduced body weight had

also been observed in the adult $Cbx3^{hypo/hypo}$ mice described previously (Brown and Singh, unpublished).

Stomachs of PP1 $Cbx3^{hypo/hypo}$ pups frequently contained no milk (*C.f.* figure 4a with 4d) and most were found dead or dying at around noon of PP1 at the periphery of the group/huddle of littermates. Death also occurred when competing wild-type and heterozygous littermates had been removed. Only three $Cbx3^{hypo/hypo}$ pups survived beyond PP1: one pup died on PP2, and two pups from one litter were sacrificed on PP8 for analysis. The mortality of the $Cbx3^{hypo/hypo}$ homozygotes was too early to be explained by non-feeding alone because non-feeding mice that do not suckle die within a time window of 12–24 h after birth (Turgeon and Meloche 2009).

External examination of $Cbx3^{hypo/hypo}$ pups provided no explanation for the severe neonatal mortality. $Cbx3^{hypo/hypo}$ newborns possessed neither the characteristic $Cbx1^{-/-}$ hunch-back phenotype (Aucott *et al.* 2008), nor any cyanosis. They also exhibited a normal righting reflex and were not anosmic. Internal examination of $Cbx3^{hypo/hypo}$, $Cbx3^{hypo/+}$ and control wild-type PP1 pups revealed no obvious malformation of organ systems necessary for postnatal survival, such as heart and kidneys. However, we consistently observed reduced vascularization of the intestines and the intrascapular BAT in $Cbx3^{hypo/hypo}$ pups (not shown). Vascularization of the intestines largely occurs postnatally and is induced by milk uptake; notably, as shown in figure 4a and d, milk was frequently absent from the stomachs of PP1 $Cbx3^{hypo/hypo}$ pups. BAT is the main site of thermogenesis in neonatal mice and vascularization of this tissue is required because of the high oxygen demands of this process (Crandall *et al.* 1997; Lim *et al.* 2012). The changes in vascularization of the intestines and BAT prompted us to examine defects in metabolism and energy homeostasis as the cause of the neonatal mortality because such defects may result in neonatal mortality in the absence of overt morphological abnormalities (Turgeon and Meloche 2009).

3.5 $Cbx3^{hypo/hypo}$ neonates are hypoglycemic and have reduced amounts of glycogen

Blood glucose measurements showed that PP1 $Cbx3^{hypo/hypo}$ neonates had significantly lower blood glucose levels than wild-type or heterozygous pups, with concentrations of 2.1 ± 0.6 mmol/L (N=9; range 3.1–<1.1) as compared to 3.1 ± 0.5 mmol/L (N=17; range 3.8–2.1; $P < 0.006$) respectively. In two of the PP1 $Cbx3^{hypo/hypo}$ pups glucose levels were below the detection limit of 1.1 mmol/L. Moderately reduced blood glucose levels were also observed in the two PP8 $Cbx3^{hypo/hypo}$ pups, even though they were found to have full stomachs upon dissection,

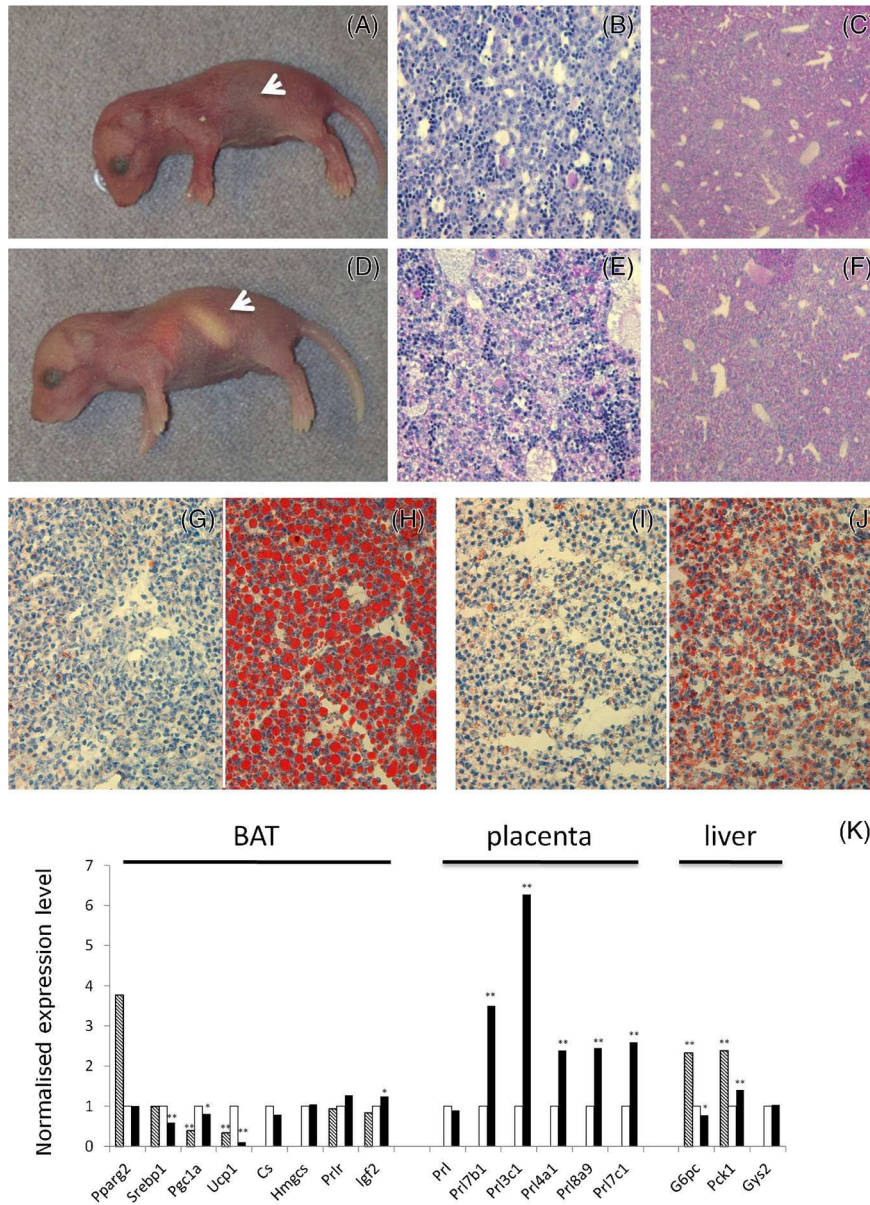


Figure 4. *Cbx3*^{hyp/hyp} neonates exhibit symptoms of defective energy homeostasis. (a) A *Cbx3*^{hyp/hyp} newborn approximately 4 h after birth. Comparison of the *Cbx3*^{hyp/hyp} newborn with its *Cbx3*^{+/+} littermate in (d) shows that the stomach of the *Cbx3*^{+/+} pup is filled with milk, as marked by the white arrow. The *Cbx3*^{hyp/hyp} newborn's stomach is empty (see white arrow). (b to f) Liver glycogen was stained with PAS in PP1 and E19 *Cbx3*^{hyp/hyp} and *Cbx3*^{+/+} livers. Comparing the PAS-staining of the PP1 *Cbx3*^{hyp/hyp} liver section in (b) with its PP1 *Cbx3*^{+/+} littermate in (e) shows a dramatic reduction of glycogen in the PP1 *Cbx3*^{hyp/hyp} liver. There was no difference in PAS-staining between staining between E19 *Cbx3*^{hyp/hyp} liver sections given in (c) with its E19 *Cbx3*^{+/+} littermate in (f). (g to j) BAT sections from E19 and PP1 *Cbx3*^{hyp/hyp} and *Cbx3*^{+/+} littermates were stained with lipid-specific stain Oil Red O (ORO). Comparison of ORO-stained BAT sections showed either complete absence or strong reduction of lipid in BAT sections of *Cbx3*^{hyp/hyp} both at E19 (i) and PP1 (g) as compared to E19 (j) and PP1 (h) *Cbx3*^{+/+} littermates. (k) Normalized real time PCR transcripts of genes expressed in *Cbx3*^{hyp/hyp} BAT, placenta and liver. mRNA transcripts were measured on E19 (black, filled bars) and PP1 (cross-hatched) and compared to *Cbx3*^{+/+} transcript levels that were normalized to 1.0 (empty bars). Significant expression changes are indicated by asterisks (**p*<0.05; ***p*<0.01). Statistical significance was assessed by unpaired *t*-test. Number of animals analysed: BAT for ORO - hyp/hyp=6; +/+ =6; BAT for gene expression - hyp/hyp=5; +/+ =5 for E19 and hyp/hyp=3; +/+ =4 for PP1; liver for PAS - hyp/hyp=6; +/+ =6; liver for gene expression hyp/hyp=3; +/+ =3 for E19 and hyp/hyp=4; +/+ =2 for PP1; placenta for gene expression hyp/hyp=3; +/+ =3. PCRs were repeated 3 times.

with 5.6 and 5.7 mmol/L (two $Cbx3^{hypo/hypo}$ pups) compared to 6.8 ($Cbx3^{+/+}$) and 7.5 mmol/L ($Cbx3^{hypo/+}$) in control littermates.

Staining of livers for PAS showed that there was reduced glycogen in newborn (PP1) $Cbx3^{hypo/hypo}$ (figure 4b) (N=6) livers compared to wild-type (figure 4e) (N=6). There was no difference in PAS staining of PP1 hearts (not shown) indicating that the depletion of liver glycogen is likely to be a secondary consequence to the inability of $Cbx3^{hypo/hypo}$ newborns to suckle and take on carbohydrate in the milk (figure 1a and d), which would be transported back to the liver via the intestines. This would also be consistent with the observation that depleted glycogen reserves were limited to postnatal livers because fetal (E19) $Cbx3^{hypo/hypo}$ (N=6) and wild-type (N=6) livers showed no difference in PAS staining (C.f. figure 4c with 4f).

Given the hypoglycemia and reduction in glycogen deposits in PP1 $Cbx3^{hypo/hypo}$ livers we investigated mRNA transcript levels of three genes coding for enzymes active in glucose/glycogen metabolism by qRT-PCR on days E19 and PP1. The genes were *glycogen synthase (Gys2)*, *glucose-6-phosphatase (G6pc)* and *phosphoenolpyruvate carboxykinase (Pck1)*. As shown in figure 4k *Pck1* was up-regulated in $Cbx3^{hypo/hypo}$ mutants at both E19 and PP1 by 1.4- and 2.3-fold respectively. *G6pc* transcript levels were also up-regulated 2.4-fold on PP1, but showed a moderate 0.8-fold down-regulation on E19 (figure 4k). There were no significant changes in expression of *Gys2* (figure 4k).

3.6 $Cbx3^{hypo/hypo}$ homozygotes are deficient in BAT lipid deposits

The finding that BAT vascularization is reduced in $Cbx3^{hypo/hypo}$ homozygotes indicated that the function of this tissue might be impaired. We therefore decided to examine the histology and lipid content by HE and Oil red O staining of BAT from PP1 $Cbx3^{hypo/hypo}$ and wild-type pups. HE revealed that BAT of $Cbx3^{hypo/hypo}$ mutants exhibited a higher nuclear density that was likely due to reduced cell volume (C.f. figure 4g with 4h). The difference in Oil Red O staining of PP1 $Cbx3^{hypo/hypo}$ (N=9) BAT compared to wild-type or $Cbx3^{hypo/+}$ controls (N=9) was striking. Lipid was either absent or strongly reduced in $Cbx3^{hypo/hypo}$ BAT (C.f. figure 4g with 4h); this strong reduction in lipid content could explain the decreased cell volume in $Cbx3^{hypo/hypo}$ BAT. We next asked whether the reduction of lipid was also found prenatally. Accordingly, we stained BAT of E19 $Cbx3^{hypo/hypo}$ fetuses with Oil Red O and showed that the lipid was also reduced in the BAT of E19 $Cbx3^{hypo/hypo}$ fetuses (9 mutant vs. 7 wild-type or heterozygous) (C.f. figure 4i with figure 4j). The prenatal depletion of lipid $Cbx3^{hypo/hypo}$ BAT indicates that the depletion was not caused solely by the inability to suckle.

The abnormal development of BAT prompted us to investigate real time mRNA transcription of genes involved in lipid metabolism and BAT differentiation in $Cbx3^{hypo/hypo}$ BAT. We measured mRNA transcripts of three genes involved in lipid metabolism, *Pparg2* (Jones et al. 2005), *Srebf1* (Eberlé et al. 2004) and *Hmgcs* (Goldstein and Brown 1990). For BAT differentiation we measured mRNA transcripts for *Prhr* (Budge et al. 2002), *Igf2*, *Pgc1a* (Wu et al. 1999), *Citrate synthase (Cs)* (Kloosterboer et al. 1979) and *Ucp1*. We observed similar levels of mRNA transcripts for *Pparg2* and *Hmgcs* while *Srebf1* transcription was elevated in $Cbx3^{hypo/hypo}$ BAT (figure 4k). *Hmgcs* is a target gene of SREBF1 protein (Horton et al. 2003). The lack of any change in *Hmgcs* expression indicates that *Hmgcs* may be regulated independently of SREBF1 in BAT. *Cs* is a quantitative marker for mitochondria (Kloosterboer et al. 1979) indicating that the number of mitochondria is unlikely to be changed in $Cbx3^{hypo/hypo}$ BAT. *Prhr* showed no change in expression but there was up-regulation of *Igf2* in $Cbx3^{hypo/hypo}$ BAT on E19 but not on PP1 (figure 4k). Notably, mRNA transcripts of BAT-specific thermogenic genes *Pgc1a* and *Ucp1* were significantly reduced on both E19 and PP1 (figure 4k), with *Ucp1* showing a marked 10-fold down-regulation on E19.

In addition to measuring specific transcripts in BAT we also investigated whether there was any effect of the $Cbx3^{hypo/hypo}$ mutation on placental prolactin (*Prl*) mRNA levels. We were prompted to do this because the placenta expresses *Prl* and prolactin is known to be involved in BAT development (Budge et al. 2002), so it was possible that changes in placental *Prl* expression could cause the changes in BAT. We also extended our investigation to measuring transcript levels of several members of the prolactin gene family (Wiemers et al. 2003), including *Prl3c1*, *Prl4a1*, *Prl7b1*, *Prl7c1* and *Prl8a9*. qRT-PCR showed that mRNA transcripts from the *Prl* gene were expressed at similar levels in E19 $Cbx3^{hypo/hypo}$ and wild-type placentas (figure 4k). Expression of mRNAs from all other family members was significantly up-regulated in E19 $Cbx3^{hypo/hypo}$ placentas (figure 4k). The up-regulation ranged from around a 2-fold increase for *Prl4a1*, *Prl7c1* and *Prl8a9* to 3-fold for *Prl7b1* and 6-fold for *Prl3c1*.

4. Discussion

Mammalian *Cbx* genes have non-redundant functions (reviewed in Singh 2010). This was first shown for the *Cbx1* gene where the proximate cause of the neonatal lethality of $Cbx1^{-/-}$ mice was the inability of the lungs to inflate because of defective innervations of the diaphragm (Aucott et al. 2008). Ablation of the *Cbx5* gene results in a specific silencing defect within the T-cell lineage (Allan et al. 2012) although $Cbx5^{-/-}$ mice are viable and fertile (cited in Aucott

et al. 2008). Here we show that the severe neonatal attrition seen in $Cbx3^{hypo/hypo}$ mutants likely results from an accumulation of deleterious lesions that begin during development *in utero*.

4.1 $Cbx3^{hypo/hypo}$ mutants are at a disadvantage at birth compared to wild-type

Depletion of CBX3 protein impedes fetal and placental growth. Placental growth restriction in $Cbx3^{hypo/hypo}$ conceptuses starts before the observed fetal growth restriction; $Cbx3^{hypo/+}$ placentas are intermediate in size between $Cbx3^{hypo/hypo}$ and wild-type placentas indicating a haplo-insufficiency and that placental growth is exquisitely sensitive to depletion of CBX3 protein. The first sign that $Cbx3^{hypo/hypo}$ placental weights were statistically smaller than wild-type was on E13 and correlates with both reduced cell proliferation and nuclear density within the labyrinth of the placenta, which is the site of nutrient, gas and waste exchange between the fetal and maternal blood supplies (Watson and Cross 2005). The weight disparity between $Cbx3^{hypo/hypo}$ and wild-type was greatest between E14 and E16, thereafter the placenta appears to compensate for its small size; the disparity was narrowed but was never closed. One compensatory mechanism that began at around E14 was an increase in nuclear density within the labyrinth of $Cbx3^{hypo/hypo}$ placentas. The increase in nuclear density was still manifested in E19 $Cbx3^{hypo/hypo}$ placentas and might provide a compensatory mechanism to increase interface between the fetal and maternal blood supplies.

The 'catch-up' in $Cbx3^{hypo/hypo}$ placental weight was not reflected in the trajectory of $Cbx3^{hypo/hypo}$ fetal weights during development: there is no 'catch-up' in the weight of $Cbx3^{hypo/hypo}$ fetuses during development. We did not find an increase in cell proliferation in $Cbx3^{hypo/hypo}$ heart, lung or tongue. There was one exception in that $Cbx3^{hypo/hypo}$ BAT exhibited increased cell proliferation compared to wild-type. Although unlikely to contribute significantly to overall fetal weight because of its small size the increased cell proliferation in $Cbx3^{hypo/hypo}$ BAT may represent a compensatory mechanism in an organ that is important for early postnatal life: BAT is responsible for the rapid production of heat at birth (Cannon and Nedergaard 2004).

Nutrient supply from the placenta to the fetus is not only dependent on the size of the placenta but also on its morphology, blood flow and the abundance of the various transport mechanisms. All three of these characteristics appear to be compromised in the $Cbx3^{hypo/hypo}$ mutant placentas. We observed a morphological narrowing of the placental blood vessels in late gestation $Cbx3^{hypo/hypo}$ placentas that is likely due to a reduction of the intracellular matrix surrounding the vessels; the smooth muscle appeared normal. Narrowing of placental blood vessels would reduce blood flow and thus

nutrient exchange and exacerbate any problems in transport across the placenta. Our investigation of transport mechanisms was revealing. In E19 placentas there was down-regulation of genes that promote placental growth such as the placenta-specific transcript of *Igf2*, *Igf2P0*, and *Grb10*. The reduced expression of *Igf2P0* is of interest because it is known to be important for placental growth (Constancia et al. 2002) and placental transport through regulation of genes such as *Slc38a2* that encode transporter proteins (Sferruzzi-Perri et al. 2011). Notably, the mRNA transcripts of both glucose (*Slc2a1* and *Slc2a3*) and amino-acid (*Slc38a1* and *Slc38a2*) transporters were significantly reduced showing that placental transport function is likely to be compromised in $Cbx3^{hypo/hypo}$ placentas. We directly tested transport capacity by measuring the cumulative transport of EFAs across $Cbx3^{hypo/hypo}$ and wild-type placentas. EFA transport is strictly regulated and involves several protein classes, such as FA translocases and FA transport proteins (Duttaroy 2009). Our results indicated that there was likely to be a defect in placental transport in $Cbx3^{hypo/hypo}$ placentas. Specifically, we found that $Cbx3^{hypo/hypo}$ fetuses in one of two E13 litters showed a significant reduction in the EFA:NEFA ratio and the $Cbx3^{hypo/hypo}$ heads of an E18 litter showed a reduced EFA:NEFA ratio.

The picture that emerges is that $Cbx3^{hypo/hypo}$ placentas are affected first, with abnormalities observed in placental morphology, blood supply and transport. These defects are likely to contribute to the fetal growth restriction that follows. An important player is, we suggest, the placenta-specific *Igf2P0* transcript. Down-regulation of the *Igf2P0* transcript could set in motion the growth and transport defects we observe in the $Cbx3^{hypo/hypo}$ placentas. A key experiment will be to test whether CBX3 protein binds the *Igf2P0* gene, which would support a role for CBX3 in facilitating proper elongation of *Igf2P0* transcript.

4.2 Loss of energy homeostasis in $Cbx3^{hypo/hypo}$ neonates

The small $Cbx3^{hypo/hypo}$ neonates show no overt morphological abnormalities. Reduced size cannot alone explain the severe postnatal mortality. For example, ablation of the *Igf2P0* transcript is not associated with postnatal mortality despite *Igf2P0* null newborns being even smaller than $Cbx3^{hypo/hypo}$ newborns – 69% (*Igf2P0* null mutant) (Constancia et al. 2002) vs. 78% ($Cbx3^{hypo/hypo}$ mutant). Other defects in $Cbx3^{hypo/hypo}$ mutants must be involved in the postnatal mortality. From our results there are good candidates that could contribute to the postnatal mortality of $Cbx3^{hypo/hypo}$ newborns.

One of the observations was that there was a likely disruption of glucose/glycogen metabolism in $Cbx3^{hypo/hypo}$ mutants. Any hypoglycemia would have been compounded by the lack of suckling of PP1 $Cbx3^{hypo/hypo}$ pups that would in turn lead

to depletion of liver glycogen reserves. The compensatory up-regulation of *G6pc* on PP1 was ineffectual because there were little glycogen reserves upon which the enzyme could act. The up-regulation of liver *Pck1*, whose product is the rate limiting step of gluconeogenesis from non-carbohydrate sources (Chakravarty et al. 2005), on E19 and PP1 was also insufficient to alleviate the hypoglycemia. We also observed a dramatic depletion of lipid stores in BAT and the reduced expression of two BAT-specific thermogenic genes, *Pgc1a* and *Ucp1*. *Pgc1a* is involved in activation of the *Ucp1* gene in BAT (Puigserver et al. 1998) and, importantly, the UCP1 protein is responsible for non-shivering thermogenesis in BAT (Matthias et al. 2000). We did not observe any changes in expression of the prolactin (*Prl*) gene in the placenta or of the gene encoding its cognate receptor (*Prlr*) in BAT, both of which are involved in BAT differentiation (Budge et al. 2002; Viengchareun et al. 2008). We did observe changes in placental expression in other members of the prolactin gene family but it is unclear what this means for BAT differentiation.

Given the broad euchromatic distribution of CBX3 (Horsley et al. 1996) and its role in transcriptional elongation of mRNA transcripts (Vakoc et al. 2005; Hediger and Gasser 2006), depletion of CBX3 is likely to have widespread effects on decreasing transcriptional elongation of many genes. Accordingly, CBX3 depletion may explain the down-regulation of mRNAs for growth regulators, *Igf2P0* and *Grb10*, glucose (*Slc2a1* and *Slc2a3*) and amino-acid (*Slc38a1* and *Slc38a2*) transporters in the placenta. The dramatic reduction of the *Ucp1* mRNA transcripts in BAT is of particular significance, especially in the context of the depleted lipid stores. This is because UCP1 protein is responsible for non-shivering thermogenesis in BAT (Matthias et al. 2000). UCP1 increases the conductance of the inner mitochondrial membrane so that BAT mitochondria generate heat instead of ATP (Nicholls and Locke 1984). There is also an essential requirement of long chain fatty acids (LCFA) in this process. UCP1 is a LCFA anion/H⁺ symporter and has an absolute requirement for LCFA in order to function (Fedorenko et al. 2012). Thus the dramatic decrease in transcription of *Ucp1* and the almost complete loss of lipid stores would render the heat-generating capacity of *Cbx3*^{hypo/hypo} BAT practically negligible.

The mechanism by which CBX3 protein activates *Ucp1* expression may be as a constituent of the PRDM16 transcriptional complex (Seale et al. 2008), which contains the histone H3K9 methyltransferase EHMT1 (Ohno et al. 2013). Depletion of CBX3 could destabilize the PRDM16 transcriptional complex in a manner that has already been described after loss of EHMT1 protein (Ohno et al. 2013). Loss of PRDM16 or EHMT1 activity decreases *Ucp1* expression to 50% and 33% of wild-type levels respectively (Seale et al. 2008; Ohno et al. 2013). By contrast *Ucp1* expression is reduced 10-fold in E19 *Cbx3*^{hypo/hypo} BAT indicating that

defects in other regulatory mechanism(s) reduce *Ucp1* expression. We suggest that inhibition of transcriptional elongation of *Ucp1* and its activator, *Pgc1a*, might also contribute to the decrease of *Ucp1* mRNA transcripts in *Cbx3*^{hypo/hypo} BAT.

4.3 A scenario for the severe attrition of *Cbx3*^{hypo/hypo} neonates

The severe postnatal mortality of *Cbx3*^{hypo/hypo} homozygotes is similar to that observed in newborn rats that have been subjected to experimental fetal growth restriction (FGR) (Cogneville et al. 1975). Cogneville and colleagues generated unilateral FGR by clamping the uterine artery of one uterine horn. Just as we observed for *Cbx3*^{hypo/hypo} mutants, the growth-restricted fetuses and newborn rats exhibited both reduced lipid stores in BAT and a severe postnatal mortality (Cogneville et al. 1975). It was argued that since BAT is essential for non-shivering thermogenesis in altricial newborn rodents, the postnatal depletion of lipids in BAT would lead to rapid hypothermia, inability to suckle, hypoglycemia, followed by death. However, work on mice deleted for *Prlr* (prolactin receptor gene), which causes reduced formation of BAT (Viengchareun et al. 2008), indicates that there is little requirement for BAT in postnatal survival in the mouse (Nadine Binart, personal communication), although, as expected, *Prlr*^{-/-} pups do succumb more rapidly to cold exposure than wild-type mice (Viengchareun et al. 2008).

Notwithstanding the observations with *Prlr*^{-/-} mice, we are persuaded that the scenario for neonatal death described by Cogneville et al. (1975) is similar to that which brings about the death of *Cbx3*^{hypo/hypo} homozygotes. This is because *Prlr*^{-/-} newborns are of normal size (Viengchareun et al. 2008), unlike the *Cbx3*^{hypo/hypo} pups and FGR neonates (Cogneville et al. 1975). The smaller *Cbx3*^{hypo/hypo} newborns would lose heat more rapidly compared to *Prlr*^{-/-} newborns because of the former's greater surface-to-volume ratio (the 'square-cube law'; Haldane 1926). Moreover, heat loss may be further compounded because, in addition to thermoregulation via BAT, thermoregulation in newborn altricial rodents has a behavioural component termed huddling (Alberts 1978; Sokoloff and Blumberg 2001; Harshaw and Alberts 2012). Huddling close to littermates is protective against the rapid heat loss that occurs during the brief exposure to cool ambient temperatures that isolated pups experience when the dam leaves the nest (Harshaw and Alberts 2012). Notably, in a huddle of newborns there is competition between pups and pups with functional BAT thermogenesis tend to avoid contact with pups whose BAT thermogenesis is blocked (Sokoloff and Blumberg 2001). Given that BAT development is abnormal in the smaller-than-normal *Cbx3*^{hypo/hypo} newborns, heat loss is likely to be further exacerbated by the mutants being pushed to the periphery

of the nest where they do not experience the thermoregulatory benefit of huddling.

A scenario for the postnatal mortality is that *Cbx3*^{hypo/hypo} mutants are born small and hypoglycemic, largely due to abnormalities in placental morphology, blood supply and transport. After birth, hypothermia sets in due to defective BAT-dependent non-shivering thermogenesis and the lack of huddling. The hypoglycemia is further compounded by an inability to suckle and depletion of glycogen reserves. These defects reinforce each other and are severally necessary and jointly sufficient in bringing about the demise of the majority of *Cbx3*^{hypo/hypo} newborns.

Acknowledgements

We are grateful to Drs Nadine Binart, Miguel Constância and Mike Soares for critically reading the manuscript, and to Drs Irene and Kenneth Söderhäll for their help and support. This work was supported by the University of Uppsala, Department for Organismic Biology, and by the VR grant 621-2009-5715 from the Swedish Research Council to Kenneth Söderhäll.

References

- Abe K, Naruse C, Kato T, Nishiuchi T, Saitou M and Asano M 2011 Loss of heterochromatin protein 1 gamma reduces the number of primordial germ cells via impaired cell cycle progression in mice. *Biol. Reprod.* **85** 1013–1024
- Alberts JR 1978 Huddling by rat pups: multisensory control of contact behavior. *J. Comp. Physiol. Psychol.* **92** 220–230
- Allan RS, Zueva E, Cammas F, Schreiber HA, Masson V, Belz GT, Roche D, Maison C, *et al.* 2012 An epigenetic silencing pathway controlling T helper 2 cell lineage, commitment. *Nature* **48** 7249–253
- Aucott R, Bullwinkel J, Yu Y, Shi W, Billur M, Brown JP, Menzel U, Kiousis D, *et al.* 2008 HP1-beta is required for development of the cerebral neocortex and neuromuscular junctions. *J. Cell. Biol.* **183** 597–606
- Billur M, Bartunik HD and Singh PB 2010 The essential function of HP1 beta: a case of the tail wagging the dog? *Trends. Biochem. Sci.* **35** 115–123
- Brown JP, Bullwinkel J, Baron-Luhr B, Billur M, Schneider P, Winking H and Singh PB 2010 HP1gamma function is required for male germ cell survival and spermatogenesis. *Epigenetics Chromatin* **3** 9
- Budge H, Mostyn A, Wilson V, Khong A, Walker AM, Symonds ME and Stephenson T 2002 The effect of maternal prolactin infusion during pregnancy on fetal adipose tissue development. *J. Endocrinol.* **174** 427–433
- Cannon B and Nedergaard J 2004 Brown adipose tissue: function and physiological significance. *Physiol. Rev.* **84** 277–359
- Canzio D, Larson A and Narlikar GJ 2014 Mechanisms of functional promiscuity by HP1 proteins. *Trends. Cell. Biol.* **24** 377–386
- Chakravarty K, Cassuto H, Reshef L and Hanson RW 2005 Factors that control the tissue-specific transcription of the gene for phosphoenolpyruvate carboxykinase-C. *Crit. Rev. Biochem. Mol. Biol.* **40** 129–154
- Coan PM, Vaughan OR, Sekita Y, Finn SL, Burton GJ, Constancia M and Fowden AL 2010 Adaptations in placental phenotype support fetal growth during undernutrition of pregnant mice. *J. Physiol.* **588** 527–538
- Cogneville AM, Cividino N and Tordet-Caridroit C 1975 Lipid composition of brown adipose tissue as related to nutrition during the neonatal period in hypotrophic rats. *J. Nutr.* **105** 982–988
- Constancia M, Hemberger M, Hughes J, Dean W, Ferguson-Smith A, Fundele R, Stewart F, Kelsey G, *et al.* 2002 Placental-specific IGF-II is a major modulator of placental and fetal growth. *Nature* **417** 945–948
- Crandall DL, Hausman GJ and Kral JG 1997 A review of the microcirculation of adipose tissue: anatomic, metabolic, and angiogenic, perspectives. *Microcirculation* **4** 211–232
- Duttaroy AK 2009 Transport of fatty acids across the human placenta: a review. *Prog. Lipid Res.* **48**(1) :52–61.
- Eberlé D, Hegarty B, Bossard P, Ferré P and Foufelle F 2004 SREBP transcription factors: master regulators of lipid homeostasis. *Biochimie.* **86** 839–848
- Fedorenko A, Lishko PV and Kirichok Y 2012 Mechanism of fatty-acid-dependent UCP1 uncoupling in brown fat mitochondria. *Cell* **151** 400–413
- Goldstein JL and Brown MS 1990 Regulation of the mevalonate pathway. *Nature* **343** 425–430
- Grewal SI and Elgin SC 2007 Transcription and RNA interference in the formation of heterochromatin. *Nature* **447** 399–406
- Haldane JBS 1926 'On Being the Right Size'. Harper's Magazine.
- Harshaw C and Alberts JR 2012 Group and individual regulation of physiology and behavior: a behavioral, thermographic, and acoustic study of mouse development. *Physiol. Behav.* **106** 670–682
- Hediger F and Gasser SM 2006 Heterochromatin protein 1: don't judge the book by its cover! *Curr. Opin. Genet. Dev.* **16** 143–150
- Horsley D, Hutchings A, Butcher GW and Singh PB 1996 M32, a murine homologue of Drosophila heterochromatin protein 1 (HP1), localises to euchromatin within interphase nuclei and is largely excluded from constitutive heterochromatin. *Cytogenet. Cell. Genet.* **73** 308–311
- Horton JD, Shah NA, Warrington JA, Anderson NN, Park SW, Brown MS and Goldstein JL 2003 Combined analysis of oligonucleotide microarray data from transgenic and knockout mice identifies direct SREBP target genes. *Proc. Natl. Acad. Sci. U.S.A.* **100** 12027–12032
- Jägerbauer EM, Fraser A, Herbst EW, Kothary R and Fundele R 1992 Parthenogenetic stem cells in postnatal mouse chimeras. *Development* **116** 95–102
- Jones DO, Cowell IG and Singh PB 2000 Mammalian chromodomain proteins: their role in genome organisation and expression. *Bioessays* **22** 124–137
- Jones JR, Barrick C, Kim KA, Lindner J, Blondeau B, Fujimoto Y, Shiota M, Kesterson RA, *et al.* 2005 Deletion of PPARγ in adipose tissues of mice protects against high fat diet-induced obesity and insulin resistance. *Proc. Natl. Acad. Sci. U.S.A.* **102** 6207–6212
- Kloosterboer HJ, Stoker-De Vries SA, Hulstaert CE and Hommes FA 1979 Quantitative analysis of morphological changes in

- skeletal muscle of the rat after hormone administration. *Biol. Neonate*. **35** 106–112
- Kurz H, Zechner U, Orth A and Fundele R 1999 Lack of correlation between placenta and offspring size in mouse interspecific crosses. *Anat. Embryol. (Berl)* **200** 335–343
- Lim S, Honek J, Xue Y, Seki T, Cao Z, Andersson P, Yang X, Hosaka K, et al. 2012 Cold-induced activation of brown adipose tissue and adipose angiogenesis in mice. *Nat. Protoc.* **7** 606–615
- Livak KJ and Schmittgen TD 2001 Analysis of relative gene expression data using real-time quantitative PCR and the 2(-Delta Delta C(T)) Method. *Methods*. **25** 402–408
- Matthias A, Ohlson KB, Fredriksson JM, Jacobsson A, Nedergaard J and Cannon B 2000 Thermogenic responses in brown fat cells are fully UCP1-dependent. UCP2 or UCP3 do not substitute for UCP1 in adrenergically or fatty acid-induced thermogenesis. *J. Biol. Chem.* **275** 25073–25081
- Nicholls DG and Locke RM 1984 Thermogenic mechanisms in brown fat. *Physiol Rev.* **64** 1–64
- Ohno H, Shinoda K, Ohyama K, Sharp LZ and Kajimura S 2013 EHMT1 controls brown adipose cell fate and thermogenesis through the PRDM16 complex. *Nature* **504** 163–167
- Puigserver P, Wu Z, Park CW, Graves R, Wright M and Spiegelman BM 1998 A cold-inducible coactivator of nuclear receptors linked to adaptive thermogenesis. *Cell*. **92** 829–839
- Saunders WS, Chue C, Goebel M, Craig C, Clark RF, Powers JA, Eissenberg JC, Elgin SC, et al. 1993 Molecular cloning of a human homologue of Drosophila heterochromatin protein HP1 using anti-centromere autoantibodies with anti-chromatin specificity. *J. Cell. Sci.* **104** 573–582
- Seale P, Bjork B, Yang W, Kajimura S, Chin S, Kuang S, Scime A, Devarakonda S, et al. 2008 PRDM16 controls a brown fat/skeletal muscle switch. *Nature* **454** 961–967
- Sferruzzi-Perri AN, Vaughan OR, Coan PM, Suci MC, Darbyshire R, Constanca M, Burton GJ and Fowden AL 2011 Placental-specific Igf2 deficiency alters developmental adaptations to undernutrition in mice. *Endocrinology* **152** 3202–3212
- Singh PB 2010 What is the essential interaction of HP1? *Genetika* **46** 1–6
- Smallwood A, Hon GC, Jin F, Henry RE, Espinosa JM and Ren B 2012 CBX3 regulates efficient RNA processing genome-wide. *Genome Res.* **22** 1426–1436
- Sokoloff G and Blumberg MS 2001 Competition and cooperation among huddling infant rats. *Dev. Psychobiol.* **39** 65–75
- Takada Y, Naruse C, Costa Y, Shirakawa T, Tachibana M, Sharif J, Kezuka-Shiotani F, et al. 2011 HP1gamma links histone methylation marks to meiotic synapsis in mice. *Development* **138** 4207–4217
- Turgeon B and Meloche S 2009 Interpreting neonatal lethal phenotypes in mouse mutants: insights into gene function and human diseases. *Physiol. Rev.* **8** 91–26
- Vakoc CR, Mandat SA, Olenchok BA and Blobel GA 2005 Histone H3 lysine 9 methylation and HP1gamma are associated with transcription elongation through mammalian chromatin. *Mol. Cell.* **19** 381–391
- Viengchareun S, Servel N, Feve B, Freemark M, Lombes M and Binart N 2008 Prolactin receptor signaling is essential for perinatal brown adipocyte function: a role for insulin-like growth factor-2. *PLoS One* **3** E1535
- Watson ED and Cross JC 2005 Development of structures and transport in the mouse placenta. *Physiology* **20** 180–193
- Wiemers DO, L-j S, Ain R, Dai G and Soares MJ 2003 The mouse prolactin gene family, locus. *Endocrinology* **144** 313–325
- Wood C, Kabat EA, Murphy LA and Goldstein IJ 1979 Immunological studies of the combining sites of the two isolectins, A4 and B4, isolated from *Bandeiraea simplicifolia*. *Arch. Biochem. Biophys.* **198** 1–11
- Wreggett KA, Hill F, James PS, Hutchings A, Butcher GW and Singh PB 1994 A mammalian homologue of Drosophila heterochromatin protein 1 (HP1) is a component of constitutive heterochromatin. *Cytogenet. Cell. Genet.* **66** 99–103
- Wu L, de Bruin A, Saavedra HI, Starovic M, Trimboli A, Yang Y, Opavska J, Wilson P, et al. 2003 Extra-embryonic function of Rb is essential for embryonic development and viability. *Nature* **421** 942–947
- Wu Z, Puigserver P, Andersson U, Zhang C, Adelmant G, Mootha V, Troy A, Cinti S, et al. 1999 Mechanisms controlling mitochondrial biogenesis and respiration through the thermogenic coactivator PGC-1. *Cell*. **98** 115–124
- Yu Y, Singh U, Shi W, Konno T, Soares MJ, Geyer R and Fundele R 2008 Influence of murine maternal diabetes on placental morphology, gene expression, and function. *Arch. Physiol. Biochem.* **114** 99–110
- Zechner U, Hemberger M, Constanca M, Orth A, Dragatsis I, Luttes A, Hameister H and Fundele R 2002 Proliferation and growth factor expression in abnormally enlarged placentas of mouse interspecific hybrids. *Dev. Dyn.* **224** 125–134

MS received 11 November 2014; accepted 16 March 2015

Corresponding editor: SANJEEV KHOSLA